Dynamic Model of Biomolecular Diffusion through Two-Dimensional Nanochannels

Carlo Cosentino,*,† Francesco Amato,† Robbie Walczak,‡ Anthony Boiarski,‡ and Mauro Ferrari§

Department of Experimental and Clinical Medicine, Università degli Studi Magna Græcia di Catanzaro, via T. Campanella 115, 88100 Catanzaro, Italy, iMEDD, Inc., 1381 Kinnear Road, Columbus, Ohio 43212, and Department of Internal Medicine, Ohio State University, 1654 Upham Drive, Columbus, Ohio 43210

Received: October 5, 2004; In Final Form: January 6, 2005

The molecular diffusion dynamics in unconstrained cases has been studied thoroughly during the last two centuries, leading to the well-known Fick's diffusion laws and Stokes−Einstein equation. More recently, a new impulse to the study of this topic has been provided by the necessity of understanding the behavior of solute particles in the presence of environmental constraints of size comparable to the molecular dimensions. In this work, we investigate the diffusion kinetics of biomolecules, such as bovine serum albumin, interferon, and lysozyme, through microfabricated silicon membranes, having pores of nanometric size in only one dimension, in the range from few to tens of nanometers (the other dimensions are in the μm range). Experimental results show that the diffusion profiles, in some cases, deviate substantially from those predicted by Fick's laws. In light of these results, a new diffusion *mathematical* model is proposed, which can reasonably explain the phenomenon and, at the same time, recovers the classical diffusion laws in the unconstrained case. Moreover, a *physical* description, derived from van der Waals equation of state, is presented, and it is compared with the results obtained by the mathematical model.

1. Introduction

Classical diffusion theory establishes that the movement of solute molecules in a nonhomogeneous solution can be predicted, from a macroscopic point of view, by Fick's laws. The basic principle is that the flux vector is proportional to the concentration gradient. Fick's laws have been successfully applied to predict the diffusion kinetics of molecules through thin semipermeable membranes.

Nevertheless, experiments have shown that, as the size of the membrane pores approaches the molecular hydrodynamic radius, unexpected effects, which cause substantial deviations from kinetics predicted by Fick's laws, can occur, as shown in ref 1 for the case of silicon nanoporous membranes. Experimental evidence of these unpredicted effects have been also observed in refs 2−7, where single file diffusion (SFD) and wall drag effect phenomena have been investigated.

In particular, in the case of SFD, the molecular flux is overestimated by Fick's law: the kinetics of SFD and Fickian diffusion are different because the molecules in SFD cannot pass each other in nanopores, regardless of the influence of concentration gradient.[8−13]

The case analyzed in ref 1 differs from those in other studies (see refs 14 and 15 and references therein), because (1) the membrane is made up of silicon and fabricated by photolithographic techniques and (2) the pores are rectangular and nanometric only in one dimension (the other dimensions are in the μm range). The observable macroscopic effect consists of a prolonged linear release of several molecules, which eventually switches to an exponential Fick's profile.

The diffusion experiments were conducted on silicon microfabricated membranes, consisting of arrays of parallel rectangular channels (Figure 1). Anchor points are interposed between the arrays, to create structural support. The channels have a width of 45 μm (the distance between two anchor points), and their length is about 4 μm. The microfabrication process allows precise tuning of the channel height in the range 7−50 nm. Due to these nanometric features achievable by this technology, nanopore membranes were originally applied to create capsules for the immunoisolation of transplanted islet cells.[16−18] In this setting, the nanopore membrane was designed to serve as the only connection between the reservoir containing the cells and the external medium. The pore height was selected to allow passage of insulin, glucose, oxygen, and carbon dioxide molecules required for proper function of the cell feedback system, while blocking elements of the immune system which might attack the graft, i.e., the transplanted islet cells.

During development of the immunoisolating biocapsule, it was noted that diffusion through nanopore membranes was slower than predicted from Fick's law when using smaller pore heights. To explore this phenomenon, the relationship between diffusion rates of various solutes, bovine serum albumin (BSA), interferon, and lysozyme, and the height of nanopore channels is investigated. In particular a new diffusion mathematical model is proposed in this work, which can provide a reasonable interpretation of the phenomenon and, at the same time, recovers the classical diffusion laws in the unconstrained case. This is a dynamic model; that is, it does not consist of a static relation (like a constant gain coefficient) between the flux and other quantities; instead it provides a relation that changes over the phenomenon evolution. The model is implemented in the Matlab-Simulink software environment[19] to run virtual experiments by means of PC-based simulations. We shall see that the simulation results fit very well the experimental data, thus

* To whom correspondence should be addressed. E-mail: carcosen@unina.it.
† Università degli Studi Magna Græcia di Catanzaro.
‡ iMEDD, Inc.
§ Ohio State University.

10.1021/jp045478u CCC: $30.25
Published on Web 03/23/2005

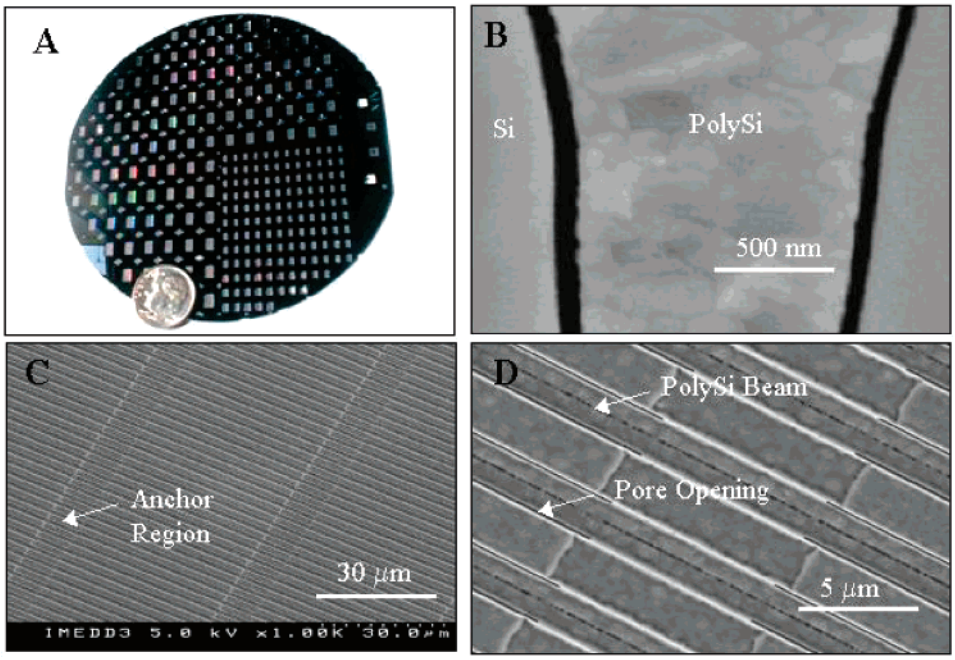

Figure 1. Photographic images of nanopore membranes. (A) Appearance of 4 in silicon wafer showing 120 small and 100 large membrane dies before being cut into individual units. (B) SEM cross-sectional view of membrane with 50 nm pores separated by silicon and poly-silicon material. (C) SEM top view of membrane with pores at 1000× magnification showing 45 μm long pores separated by 10 μm long anchor regions. (D) 6000× top SEM view of membrane showing details of pore and anchor structures. (Reproduced from ref 1).

confirming that the proposed diffusion model can give a reasonable interpretation of the non-Fickian diffusion kinetics.

To provide also a physical interpretation of the phenomenon, we will also present a *physical* model, built upon a generalization of Fick's laws and directly derived from the van der Waals equation of state.

The paper is organized as follows. Section 2 gives a novel mathematical interpretation of diffusion through nanochannels. In section 3, experimental results from ref 1 are analyzed under the light of the new theoretical results and compared with the ones predicted by classical diffusion theory. Then, Peskir's diffusion law is introduced, and the results derived by this law are compared with those obtained by the proposed model. The experimental and theoretical results are discussed and conclusions are drawn in section 4.

2. Theoretical Calculations

When there is a chemical potential gradient in a single-phase fluid mixture, which implies that a concentration gradient is present in the fluid mixture, each species will diffuse in the direction of decreasing concentration. The mathematical formula which describes this phenomenon is known as Fick's law. It represents a linear relationship between the mass (or molar) flux J_A (with respect to the mass average velocity), and the concentration gradient, ∇c_A.[21]

For a binary mixture, Fick's first law is

$$J_A = -D_{AB}\nabla c_A \tag{1}$$

where D_{AB} is the coefficient diffusion of a solute A in a solvent B.

2.1. Free Diffusion. To have a good insight of the process, we first apply the classical theory to our specific case study, but still neglecting the effect of the membrane. In the next section we will introduce the mathematical description of the membrane effect, so that we can compare this case with the free-diffusion case.

The binary mixture consists of a solvent, e.g. phosphate buffer saline (PBS), and a certain solute, which is initially concentrated in a well-defined region of the reservoir volume. To obtain a suitable model, we require the following hypotheses to hold:

(a) The experimental volume, V_T, contains a total mass M_{AT} of drug *A*; it can be divided in two compartments of volume V_1 (the reservoir) and V_2 (the sink), with the respective initial mass concentrations, $c^0_{A1} = c_{A1}(0)$ and $c^0_{A2} = c_{A2}(0)$ ($c^0_{A1} > c^0_{A2}$).

(b) The concentration is homogeneous in each compartment and the concentration variation is spatially defined in a thin boundary region of depht *L*.

(c) Given a Cartesian reference system (*x*, *y*, *z*), the concentration gradient,∇c_A, has null components along the *y* and *z* axes.

Our aim is to calculate the mass flux of drug through a generic surface, of area *S*, which we assume to be perpendicular to the diffusion path.

From 1, taking into account the hypotheses (b) and (c), we can approximate the flux as

$$J_A(t) = D_{AB}\frac{c_{A1}(t) - c_{A2}(t)}{L} \tag{2}$$

Since the concentration profile in the boundary region between V_1 and V_2 is not precisely defined, we approximate the concentration derivative along *x* with the ratio of the extreme values difference and the diffusion depth *L*.

Denoted by $c_{A1}(t)$ and $c_{A2}(t)$ the mass concentrations at time *t* in the two compartments, the conservation principle yields for all *t*

$$c_{A1}(t)V_1 + c_{A2}(t)V_2 = M_{AT}\ (=c^0_{A1}V_1 + c^0_{A2}V_2) \tag{3}$$

thus, the concentration in one of the two compartments can be expressed as a function of the other as follows:

$$c_{A2}(t) = \frac{M_{AT}}{V_2} - \frac{V_1}{V_2} c_{A1}(t) \tag{4}$$

On the other hand, the application of the conservation principle on a small time interval $(t,t + \Delta t)$ yields

$$-\int_t^{t+\Delta t} J_A(\tau) S \, d\tau = V_1 \Delta C_{A1} \tag{5}$$

By dividing both sides of 5 by Δt and taking the limit for $\Delta t \rightarrow 0$, we obtain a relation between the concentration derivative with respect to time, $\dot{c}_{A1}(t)$, and the mass flux

$$\dot{c}_{A1}(t) = -J_A(t)\frac{S}{V_1} \tag{6}$$

Taking into account 2 and 4, the concentration derivative varies according to the following relation:

$$\dot{c}_{A1}(t) = -\frac{D_{AB}S}{V_1 L}\left(1 + \frac{V_1}{V_2}\right) c_{A1}(t) + \frac{D_{AB}S}{V_1 V_2 L} M_{AT} \tag{7}$$

and, solving the differential equation, we obtain

$$c_{A1}(t) = c_{A1}^0 e^{-\lambda_A t} + \frac{M_{AT}}{V_1 + V_2}(1 - e^{-\lambda_A t}) \tag{8}$$

where $\lambda_A = (D_{AB}S/V_1 L)[1 + (V_1/V_2)]$.

Substitution of 8 into 2, taking into account 3, yields

$$J_A(t) = (c_{A1}^0 - c_{A2}^0)\frac{D_{AB}}{L} e^{-\lambda_A t} \tag{9}$$

Therefore, in the free diffusion case, the release profile is exponential.

At this point, we can also calculate the amount of drug A, $Q_A(t)$, which passes from V_1 to V_2 over an arbitrary time interval $[0,t]$, by integrating the mass flux times the area, S, thus obtaining

$$Q_A(t) = \int S J_A(t) \, dt = (c_{A1}^0 - c_{A2}^0)\frac{V_1 V_2}{V_1 + V_2}(1 - e^{-\lambda_A t}) \tag{10}$$

2.2. Diffusion through Nanochannels. Now let us derive the constrained diffusion model. Experimental results in ref 1 show that the release profile remains linear for a certain period, and then it switches to the Fickian exponential trend. This observation suggests that the theory developed in the previous subsection for the unconstrained case can still be suitable, whereas the linear release can be described by simply adding further terms or modifying some function in the previous mathematical relations, instead of starting from first principles.

Having this in mind, we hypothesize that the effect of the membrane can be modeled by means of a saturation effect on the mass flux, so that relation 2 now becomes

$$J_A(t) = sat\left[\frac{D_{AB}}{L}(c_{A1}(t) - c_{A2}(t))\right]_{-\hat{J}_A}^{\hat{J}_A} \tag{11}$$

where $\hat{J}_A$ is the saturation threshold and the saturation function has been defined as

$$sat[x]_a^b = \begin{cases} b \text{ if } x > b \\ x \text{ if } x \in [a,b] \\ a \text{ if } x < a \end{cases}$$

This hypothesis is fairly reasonable, because we can think of each nanochannel as a bottleneck: Over a certain concentration level, the molecular flux through the channel will remain the same regardless of the number of particles per unit volume in the reservoir compartment.

Moreover this description coincides with the classical diffusion laws if we let the threshold value be very large (which means unconstrained diffusion). Finally, the switch between the linear and exponential diffusion can be simply explained by the fact that the concentration decreases in the reservoir, eventually yielding the concentration gradient (and therefore the flux) to return below the threshold value.

Indeed, substituting J_A in (3) and using the new expression given by (11), we obtain that two different evolution laws are possible, depending on the concentration value:

(i) Constrained diffusion: If $|c_{A1}(t) - c_{A2}(t)| > \hat{J}_A L/D_{AB}$, we have

$$\dot{c}_{A1}(t) = -\frac{\hat{J}_A S}{V_1} \tag{12}$$

and the release profile is linear.

(ii) Free diffusion: If $|c_{A1}(t) - c_{A2}(t)| \leq \hat{J}_A L/D_{AB}$, the evolution laws will be the same ones derived in the previous section, exhibiting an exponential release profile.

We can calculate the settling time, T_{a1}, defined as the time the concentration $c_{A1}(t)$ needs to reach the final value with a tolerance of 1%. In the free-diffusion case the release profile is exponential and, from systems theory, it is well-known that[22]

$$T_{a1} = \frac{4.6}{\lambda_A} = 4.6\frac{L}{SD_{AB}}\frac{V_1 V_2}{(V_1 + V_2)} \tag{13}$$

In the case of constrained diffusion we are more interested in calculating the duration of the linear release period: Assuming that the initial concentration difference is large enough such to cause the flux saturation at the value $\hat{J}_A$, the concentration variation is described by the linear relation

$$c_{A1}(t) = c_{A1}^0 - \frac{\hat{J}_A S}{V_1} t \tag{14}$$

in the time interval $[0,T_F]$, where T_F denotes the end of the linear release interval. Then the saturation effect vanishes and the diffusion is again described by Fick's law. The value T_F can be easily found to be

$$T_F = \frac{c_{A1}^0 V_1}{\hat{J}_A S} - \frac{V_1 V_2}{\hat{J}_A S(V_1 + V_2)}\left(\frac{M_{AT}}{V_2} + \frac{\hat{J}_A L}{D_{AB}}\right) \tag{15}$$

which derives from 11 and 14.

3. Discussion

3.1. Interpretation of the Experimental Data. Hereafter we will exploit the model developed in the previous section to interpret some experimental results presented in ref 1. The biomolecules considered in ref 1 are interferon α−2b, lysozyme and bovine serum albumine (BSA), since they are useful in the therapeutic treatment of some diseases; for example, the administration of interferon alpha-2b has been proven to be useful in the treatment of chronic hepatitis C, whereas lysozyme has exhibited preventive and therapeutic antitumor activity.

The release profile obtained from human recombinant interferon α−2b (19 kDa) diffusion experiments is shown in Figure

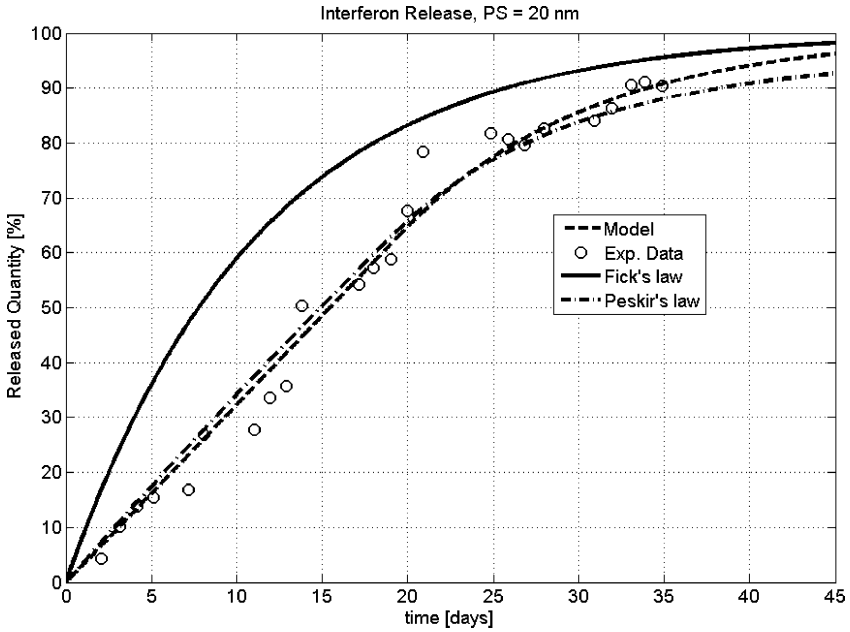

Figure 2. In vitro interferon diffusion through nanopore membrane (20 nm pore height) under sink conditions: experimental data (○), Fick's law (—), model based simulation (– – –), Peskir's law (– · – · – ·).

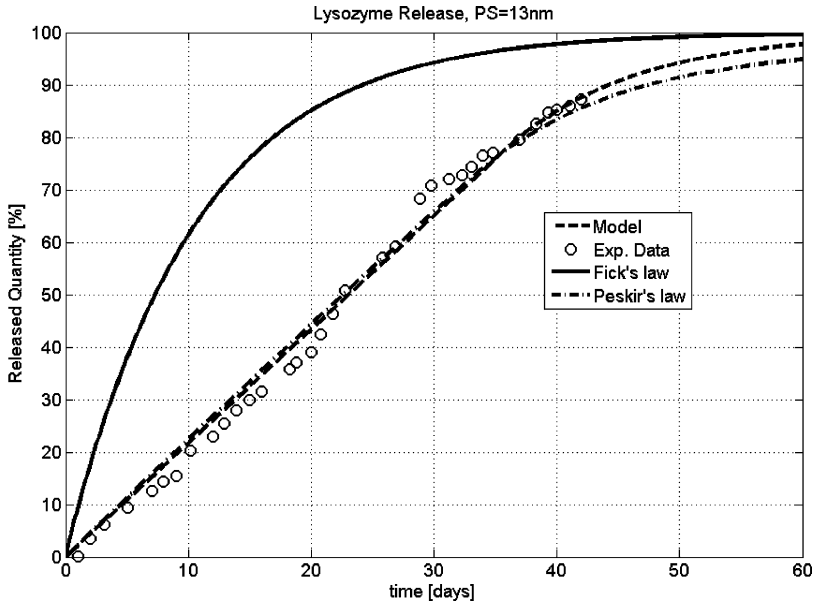

Figure 3. In vitro lysozyme diffusion through nanopore membrane (13 nm pore height) under sink conditions: experimental data (○), Fick's law (—), model based simulation (– – –), Peskir's law (– · – · – ·).

2. The membrane used in the experiment had a 20 nm pore height, the initial concentration in the donor well was 4.68 mg/mL. Figures 3 and 4 show the results of the same kind of sink-condition ($C_{A2} \approx 0$) diffusion test repeated with lysozyme (14 kDa) and bovine serum albumine (67 kDa) respectively; the initial concentration in both cases is 5 mg/mL, and the pore height 13 nm. The solvent used in all of the experiments is PBS. Although lysozyme release data have not been shown in ref 1, the reader can refer to materials and methods reported there, which are similar to the ones used for lysozyme diffusion experiments. In all of these three cases, it is evident how the diffusion profile estimated by Fick's law (solid lines) is completely different from the experimental one (circle markers). Moreover, it is important to note that, even if the experimental parameter values were varied, Fick's law could not explain the experimental data, because the initial part of the release curve is almost linear, which is not in agreement with classical diffusion theory. This behavior, instead, agrees with the nanochannel diffusion model developed in section 2 (dashed lines), which provides a good fit of the data before and after the "switch" to the Fickian behavior (the results represented by dash−dot lines will be discussed in the next section).

The phenomenon is further explained in Figure 5: the diagrams show the nominal mass flux predicted by Fick's laws (solid line), compared with that computed by the model (dashed line) for the interferon diffusion experiment. The saturation effect, which appears evident in this figure, does not only keep the flux constant but also increases the release period. Moreover, it is easy to understand that, taking a certain amount of drug, the larger the initial concentration, the longer the linear release period, as stated also by relation 15. The reason is that the period of linear release mainly depends on the gap between the initial and the saturation threshold concentration.

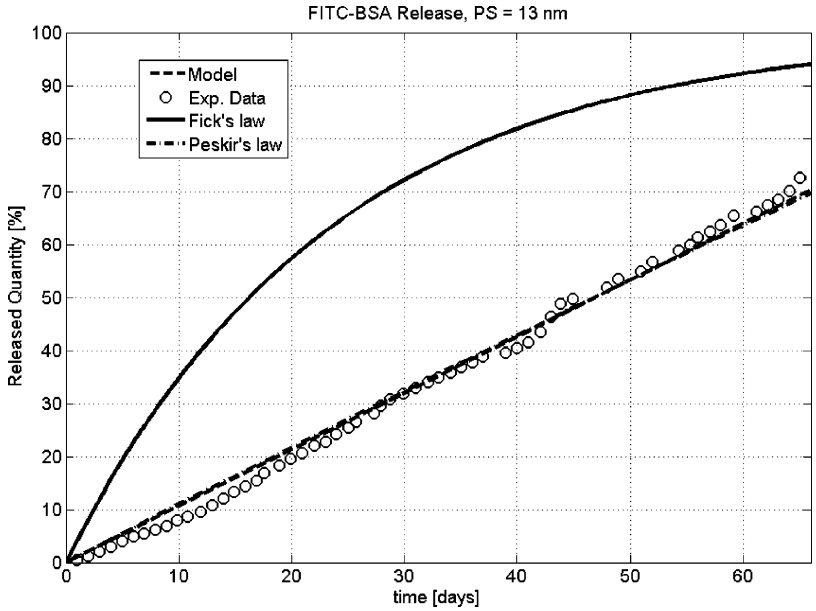

Figure 4. In vitro diffusion kinetics of fluorescein isothiocyanate (FITC) labeled-BSA through 13 nm pore height membrane under sink conditions: experimental data (○), Fick's law (—), model based simulation (− − −), Peskir's law (− · − · − ·).

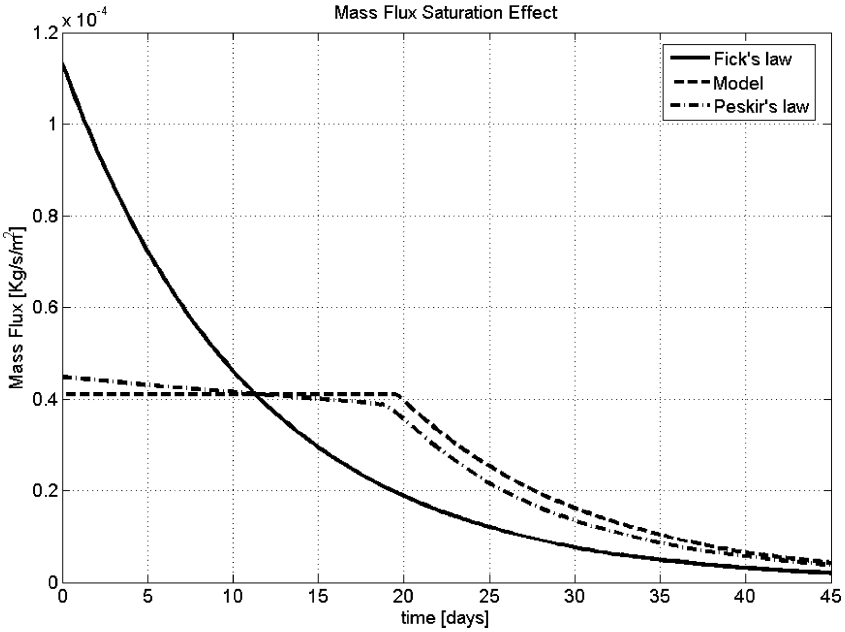

Figure 5. Interferon mass flux through a 20 nm pore height membrane: Fick's law prediction (—), model based simulation (− − −).

TABLE 1: Experimental Data Fitting Results

molecule	pore height [nm]	Init. conc. [mg/mL]	D_{AB} [cm^2/s]	$\hat{J}_A$ [Kg/m^2/s]
interferon	20	4.68	9.60×10^{-7}	4.08×10^{-5}
lysozyme	13	5.00	1.07×10^{-6}	3.05×10^{-5}
BSA	13	5.00	6.39×10^{-7}	1.89×10^{-5}

An optimization routine has been set up in order to identify the value of the saturation threshold flux parameter, $\hat{J}_A$, in the various cases discussed above (Table 1). The model devised in section 2 has been implemented in Matlab/Simulink and the flux saturation parameter has been optimized in order to obtain the best match between the model predicted release profile and the experimental data. Note that it is the only tunable parameter of the model that must be experimentally identified.

3.2. Physical Interpretation. The model presented in section 2.2 has been devised as a mathematical tool for fitting the experimental data, and for predicting the behavior of molecular diffusion with respect to variation of the governing parameters.

However, to this point no explanation has been provided about the physical principles which give origin to the phenomena under consideration. This section will be devoted to present a physical interpretation of the non-Fickian behavior observed in the diffusion experiments described above.

Classical diffusion studies are based on Fick's first law and on the Einstein's relation, which expresses the diffusion coefficient of spherical Brownian particles in a solution as

$$\mathrm{DAB} = \frac{kT}{6\pi r\eta} \tag{16}$$

where k is the Boltzmann constant, T is the temperature, r is the radius of the solute particles, and η is the viscosity coefficient of the liquid.

As a starting point, we shall consider changes in the diffusion coefficient when the equation of state of Brownian particles in

TABLE 2: Experimental Data Fitting Results

molecule	pore height [nm]	init. conc. [mg/mL]	a [Pa m^6]	b [m^3]
interferon	20	4.68	2.68×10^3	6.51
lysozyme	13	5.00	4.51×10^3	3.99
BSA	13	5.00	23.1×10^3	13.9

the Einstein argument deviates from the ideal gas law to the van der Waals equation

$$\left(p + \frac{a}{\gamma^2}\right)(\gamma - b) = RT \tag{17}$$

where p is the pressure, R is the universal gas constant, and $\gamma = V/n$ is the molar volume. It is well-known that the constants a and b, though their values are experimentally identified, have a physical interpretation: The term a/γ^2 represents the additional positive pressure caused by the presence of other solute particles, as a consequence of the long-range attractive forces; the constant b, instead, represents the volume occupied by the gas molecules, so that $\gamma - b$ represents the effective "free volume".

In the following, we will exploit the work of Peskir,[23] who derived from (17) the following generalized expression for the diffusion coefficient [compare with (16)]

$$\tilde{D}_{AB} = \frac{kT}{6\pi r\eta}\left[\frac{1}{(1 - b_0\nu)^2} - \frac{2a_0}{kT}\nu\right] \tag{18}$$

where $\nu = \nu(t,x)$ is the average number of Brownian particles at position x at time t, $a_0 = a/N_0^2$, $b_0 = b/N_0$, and N_0 is the Avogadro's number. Note that the generalized coefficient $\tilde{D}_{AB}$ recovers the Einstein coefficient D_{AB} when $a = b = 0$.

It is important to note that, according to (18), the diffusion coefficient is an increasing function of b, and a decreasing function of a. This is intuitively what we could expect, because the value of a is determined by long-range *attractive* forces, which oppose to particles' dispersion, whereas the value of b is related to the short range *repulsive* forces, which foster particles dispersion.

The generalized expression 18 also allows us to derive the effect of temperature and pressure variations on the diffusion coefficient: A temperature increase corresponds to a larger diffusion coefficient; conversely, a pressure increase has the opposite effect.

The expression 18 yields the following relation:[23]

$$\frac{\partial\nu}{\partial t} = \left(\frac{kT}{m\beta}\frac{2b_0}{(1 - b_0\nu)^3} - \frac{2a_0}{m\beta}\right)\left(\frac{\partial\nu}{\partial x}\right)^2 + \left(\frac{kT}{m\beta}\frac{1}{(1 - b_0\nu)^2} - \frac{2a_0}{m\beta}\nu\right)\frac{\partial^2\nu}{\partial x^2} \tag{19}$$

which is a generalized diffusion law (it recovers Fick's second law of diffusion in the case $a = b = 0$).

A finite-element model has been built upon relation 19; the corresponding van der Waals coefficients have been identified for each of the experiments presented in the previous sections, by means of data interpolation. Figures 2−4 show the data fitting by the physical model, whereas Figure 5 shows the reconstructed mass flux for the diffusion experiment with interferon (dash−dot lines). It is relevant to note that the results obtained by the mathematical model are very similar to those obtained by Peskir's law.

The van der Waals coefficients, identified by fitting the experimental data, are reported in Table 2.

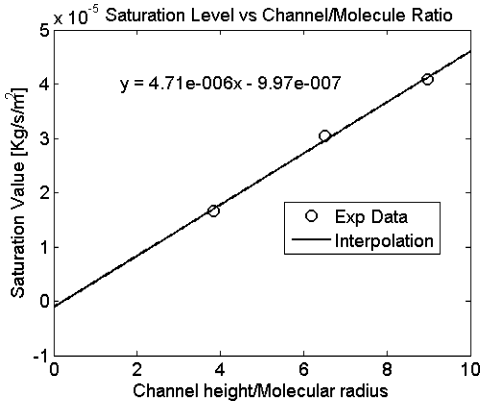

Figure 6. Flux saturation threshold as a function of channel height/molecular radius ratio.

3.3. Relevance of the Results. Peskir's law yields a *physical* interpretation of the molecular diffusion through silicon nanochannels, because it is based on van der Waals equation. Nevertheless, the model exploiting Peskir's law is in principle not so different from the *mathematical* model presented in section 2.2. Indeed, both models require the evaluation of some experimental parameters (one in the case of the mathematical model, two in the case of the Peskir's law).

On the other hand, the mathematical model exhibits a lower complexity, since, as said, it is dependent on only one parameter; therefore, it seems more suitable for a simple macroscopical analysis of the experimental data.

The results obtained can be used to predict the diffusion of different molecules, given the channel height. To this aim, a linear relation has been found by interpolation (Figure 6), which expresses the flux saturation threshold as a function of the ratio of the channel height and the Stokes' radius of the solute. A consideration is opportune, regarding the relation drawn in Figure 6: If we considered ideally the molecule as a rigid sphere, the volume would increase proportionally to the cube of the radius, that is $V = 4\pi r^3/3$.

For this reason, we would expect the relation in Figure 6 to have a cubic shape. However, it must be taken into account that the nanochannels constrain the Brownian motion only in one dimension; therefore, we could expect the diffusion to increase linearly with the channel height for a given molecule. This consideration supports the validity of the data shown in Figure 6, though this relation must be investigated further, by analyzing more experimental data.

The results discussed above suggest that nanopore membranes can be engineered to control diffusion rates and kinetic order by "fine-tuning" channel height in relation to the size of solutes. Moreover, when the proper balance is struck, zero-order diffusion kinetics is possible. Implantable zero-order output devices are useful to deliver drugs which are not orally bioavailable, particularly in clinical settings, where maintenance of a steady-state level in the blood stream for long periods is desirable.[24]

On the basis of these results we can also conclude that the total molecular flux through the membrane can be controlled by varying the porosity and the total porous area, whereas the diffusion kinetics can be controlled by changing the channel height.

3.4. Comparison to Other Known Diffusion Phenomena. Non-Fickian diffusion has been already observed experimentally, in particular in the case of adsorbate molecules such as methane and CF_4 in crystalline zeolites, where SFD occurs.[5] Another phenomenon which cannot be described by classical diffusion

theory is the motion of colloidal particles in a density matched fluid confined between two flat plates: in this case, diffusion is hindered by hydrodynamic drag effects at distances close to the walls, as evidenced in ref 25.

The phenomenon analyzed here differs from the aforementioned ones, because the microfabricated nanopore channels used here are of molecular size in only one dimension and the solutes themselves do not tend to adsorb to the silicon surface. The basic principle of diffusion as a mixing process with solutes free to undergo Brownian motion in three dimensions does not apply since in at least one dimension solute movement within the nanopore is physically constrained by the channel walls. However, unlike the SFD case, the ordering of solute particles imposed by the nanopore geometry is not as strict as true cylindrical pores, but particles could conceivably pass each other laterally. Furthermore, the wall drag effect has been evidenced using plastic micro-sphere moving into microchannels, which could be significantly different from the case of low weight molecules diffusing in nanochannels.

Whether a consequence of a SFD-like phenomenon or drag effects (or a combination of both), the nanopore membrane used here is rate-limiting and, if properly tuned, restricts solute diffusion to a point that flux rate across the membrane is entirely independent of the concentration gradient.

4. Conclusions

The experimental results presented in ref 1 prove that the diffusion kinetics through nanochannels cannot be described by classical Fick's laws. A novel mathematical description has been formulated, on the basis of the *flux saturation* assumption, and the simulation results have shown that this model is suitable for explaining the non-Fickian diffusion.

Moreover, a physical model has been also given, based on Peskir's law of diffusion (which, in turn, builds upon van der Waals relation), and the results have been shown to match those obtained by the mathematical model.

Understanding the mechanism of diffusion through nanochannels is important not only from a theoretical perspective, but also in view of the potential applications of nanopore silicon membranes: The release rate has been shown to be constant for a long period, under suitable choice of the experimental parameters (initial concentration, channel height and size of solutes); this property can be exploited in clinical medicine for prolonged and constant administration of drugs; in this case it is of paramount importance to have a quantitative method for the device tuning and the prediction of the amount of drug released in the patient within a certain time period. Furthermore, the model could also be used as a tool for quality control of the membranes fabrication process, which, at present, represents a difficult task to perform in a nondestructive way.

References and Notes

(1) Martin, F.; Walczak, R.; Boiarski, A.; Cohen, M.; West, T.; Cosentino, C.; Ferrari, M. *J. Controlled Release* **2005**, *102*, 123.
(2) Clark, L. A.; Ye, G. T.; Snurr, R. Q. *Phys. Rev. Lett.* **2000**, *84*, 2893.
(3) Meersmann, T.; Logan, J. W.; Simonutti, R.; Caldarelli, S.; Comotti, A.; Sozzani, P.; Kaiser, L. G.; Pines, A. *J. Phys. Chem. A* **2000**, *104*, 11665.
(4) Wei, Q.; Bechinger, C.; Leiderer P. *Science* **2000**, *287*, 625.
(5) Kukla, V.; Kornatowski, J.; Demuth, D.; Girnus, I.; Pfeifer, H.; Rees, L. V. C.; Schunk, S.; Unger, K. K.; Karger, J. *Science* **1996**, *272*, 702.
(6) Gupta, V.; Nivarthi, S. S.; Keffer, D.; McCormick, A. V.; Davis, H. T. *Science* **1996**, *274*, 164.
(7) Hahn, K.; Karger, J.; Kukla, V. V. *Phys. Rev. Lett.* **1996**, *76*, 2762.
(8) Auerbach, S. M. *Int. Rev. Phys. Chem.* **2000**, *19*, 155.
(9) Mao, Z.; Sinnott, S. B. *J. Phys. Chem. B* **2000**, *104*, 4618.
(10) Nelson, P.; Auerbach, S. *J. Chem. Phys.* **1999**, *110*, 9235.
(11) MacElroy, J. M. D.; Suh, S. H. *J. Chem. Phys.* **1997**, *106*, 8595.
(12) Aityan, S. K.; Portnov, V. I. *Gen. Physiol. Biophys.* **1986**, *5*, 351.
(13) Levitt, D. G. *Phys. Rev. A (Gen. Phys.)* **1973**, *8*, 3050.
(14) Nakao, S. *J. Membrane Sci.* **1994**, *96*, 131.
(15) Peppas, N. A.; Meadows, D. L. *J. Membrane Sci.* **1983**, *16*, 361.
(16) Desai, T. A. *Expert Opin. Biol. Ther.* **2002**, *2*, 633.
(17) Desai, T. A.; Chu, W. H.; Tu, J. K.; Beattie, G. M.; Hayek, A.; Ferrari, M.*Biotechnol. Bioeng.* **1998**, *57*, 118.
(18) Desai, T. A.; Hansford, D.; Ferrari, M. *J. Membrane Sci.* **1999**, *159*, 221.
(19) *[19]Simulink user's guide: Dynamic system simulation for MATLAB*; The MathWorks, Inc.: Natick, MA, 1997.
(20) Chu, W. H.; Chin, R.; Huen, T.; Ferrari, M. *J. Microelectromech. Syst.* **1999**, *8*, 34.
(21) Saatdjian, E. *Transport Phenomena Equations and Numerical Solutions*; Wiley & Sons: New York, 2000; Chapter 3.
(22) Franklin, G. F.; Powell, J. D.; Emami-Naeini, A. *Feedback Control of Dynamic Systems*, 4th ed.; Prentice Hall: Upper Saddle River, NJ, 1994; Chapter 3.
(23) Peskir, G. *Stoch. Models* **2003**, *19*, 383.
(24) Wright, J. C.; et al. *J. Controlled Release* **2001**, *75*, 1.
(25) Lin, B.; Yu, J.; Rice, S. *Phys. Rev. E* **2000**, *62*, 3909.